Chemical Physics 53 (1980) 265–277

THE RYDBERG STATES OF TRANS-1,3,5-HEXATRIENE FROM AB INITIO AND CONFIGURATION INTERACTION CALCUEATIONS*

Marco A.C. NASCIMENTO
Instituto de Quimica, Departamento de Fisico-Quimica, Universidade Federal do Rio de Janeiro, Rio de Janeiro, Brasil

and

William A. GODDARD III
Arthur Amos Noyes Laboratory of Chemical Physics†, California Institute of Technology, Pasadena, California 91125, USA

Received 6 June 1980

Self-consistent ab initio and configuration interaction (CI) calculations are presented for the Rydberg states of the *trans*-1,3,5-hexatriene molecule. Seven Rydberg series were identified, four optically allowed (ns, nd_{z^2}, $nd_{\bar{xy}}$) and three optically forbidden (np_x, $np_{\bar{y}}$, np_z). These present results plus previous calculations on the valence states are used to assign the transitions observed in the ultraviolet (UV), electron-impact (EI) and two-photon spectra of this molecule.

1. Introduction

The electronic spectra of linear polyenes have been the subject of intensive experimental [1–15] studies, mainly because they form the basic chromophore of important photobiological systems such as the visual pigments [16] and bacteriorhodopsin [17]. Various polyenes have now been studied using such techniques as vacuum-ultraviolet [2, 3, 13], electron-impact spectroscopy [4–6, 11, 14, 15], ion impact [12] and multiphoton spectroscopy [7–10]. However, there is still considerable uncertainty in both the nature and the assignment of even the smaller polyenes such as 1,3-*trans*-butadiene and 1,3,5-*trans*-hexatriene (hereafter referred to as butadiene and hexatriene, respectively).

In previous publications [18–20] (hereafter referred to as papers I, II, and III) we presented results of extensive ab initio generalized valence bond (GVB) and configuration interaction (CI) studies for the valence states of butadiene and hexatriene [18] (paper I) and for the Rydberg states of butadiene [20] (paper III).

The results obtained in this paper together with the ones of paper I are used to assign the observed one- and two-photon and electron-impact spectra of hexatriene.

* Work performed at California Institute of Technology.
† Contribution No. 6247.

2. Basis set and geometry

All the calculations reported in this paper were carried out using the Dunning [21] valence double-zeta contraction of the Huzinaga [22] double-zeta (9s/5p, 4s) gaussian basis set, augmented with diffuse basis functions of 3s, $3p_\sigma$ and $3p_\pi$ character in order to provide an adequate description of the Rydberg excited states. We used the ground state geometry, as determined experimentally by electron diffraction techniques [23], in all the calculations.

3. Hexatriene Rydberg states

In this section, we describe the calculations performed for the Rydberg states of hexatriene.

For this molecule, with six electrons in the π space, a simple MO description gives a ground state corresponding to the electronic configuration $(1a_u)^2\ (1b_g)^2\ (2a_u)^2$ plus three unoccupied orbitals $2b_g$, $3a_u$, $3b_g$ in order of increasing energy. This molecule has C_{2h} symmetry and the atomic orbitals will have symmetries $ns = a_g$; $np = a_u, b_u$; $nd = a_g, b_g$; $nf = a_u, b_u$.

The first dipole allowed state will correspond to the $2a_u \rightarrow 2b_g$ ($\pi \rightarrow \pi^*$) transition which gives rise to a ^1B_u state. As in butadiene, this state involves valence and diffuse character.

The Rydberg states for this molecule will have overall symmetries $B_g(2a_u \rightarrow np_\sigma)$, $A_u(2a_u \rightarrow ns, nd_\sigma)$, $A_g(2a_u \rightarrow np_\pi, nf_\pi)$ and $B_u(2a_u \rightarrow nd_\pi)$. Transitions to the ^1A_u and ^1B_u states are optically allowed while transitions to the ^1A_g and ^1B_g states are forbidden.

3.1. Basis set

In order to describe the σ Rydberg states we initially augmented the valence basis set with diffuse basis functions of 3s, $3p_y$ and $3p_z$ character ($\zeta_{3s} = 0.023$, $\zeta_{3p} = 0.021$) centered on each carbon atom. An IVO calculation [24] with this basis set (basis A, table 1) gives an adequate description of the 3s, $3p_\sigma$, $3p_{\sigma'}$, $3d_\sigma$, $3d_{\sigma'}$, and $3d_{\sigma''}$ Rydberg orbitals. This same basis (A) also generates $4p_\sigma$, $4f_\sigma$, and $5g_\sigma$ Rydberg orbitals. Fig. 1 shows the first three σ Rydberg orbitals generated with this basis. Figs. 2 and 3 show the 3d and the $5g_{z^4}$ Rydberg orbitals, respectively.

As for butadiene [20] we reduced the size of the basis set (without loss of accuracy) in order to perform the SCF and CI calculations. To this purpose we augmented the valence basis set with one set of 3s, $3p_y$ and $3p_z$ basis functions centered at the C_1–C_2, C_3–C_4 and C_5–C_6 bond midpoints. As we can see from table 1 (basis B) and figs 1(b, d, f), this basis set gives a very good description of the σ Rydberg states. For the π Rydberg states, the valence basis set was augmented with diffuse basis functions of $3p_x$ character ($\xi = 0.021$) centered on each carbon atom (table 1, basis C).

3.2. Character of the Rydberg orbitals

As for butadiene, the Rydberg orbitals for hexatriene very much resemble the corresponding atomic orbitals.

The σ Rydberg orbitals are oriented parallel ($\bar{z}$ axis) and perpendicular ($\bar{y}$ axis) to the long

Table 1
IVO excitation energies[a] (in eV) of hexatriene for the $\pi(2a_u) \rightarrow$ Rydberg transitions for different basis sets

Basis set augmentation[b]	No. diffuse basis functions	Excited orbital					
(a) σ Rydberg orbitals		3s	$3p_{\bar{y}}$	$3p_{\bar{z}}$	$3d_{\bar{z}^2}$	$3d_{\bar{y}\bar{z}}$	$3d_{\bar{x}^2-\bar{y}^2}$
(A) one 3s, $3p_y$ and $3p_z$ basis function on each carbon atom	18	6.32	6.37	6.73	7.15	7.26	7.50
(B) one 3s, $3p_y$ and $3p_z$ basis function on the midpoints of C_1–C_2, C_3–C_4 and C_5–C_6 bonds	9	6.43	6.42	6.75	7.23	7.30	
(b) π Rydberg orbitals		$3p_x$	$3d_{xz}$	$3d_{xy}$	$4f_{xz^2}$	$4f_{xy^2}$	$4p_x$
(C) one $3p_\pi$ basis function on each carbon atom	6	6.65	6.80	7.15	7.34	7.72	7.77

[a] Using the relation $E_i = IP - \varepsilon_i$ with IP = 8.45 eV.
[b] In all cases the gaussian exponents used are: $\xi_{3s} = 0.023$, $\xi_{3p} = 0.021$.

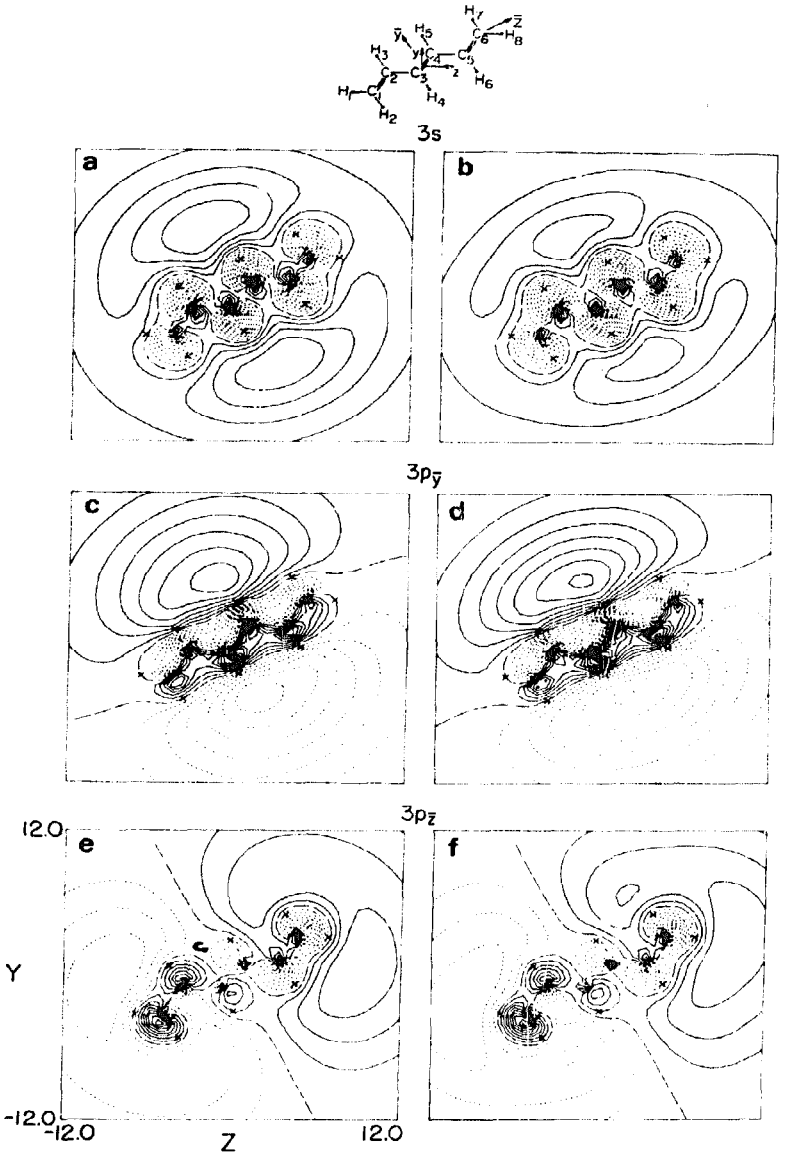

Fig. 1. 3s and 3p$_\sigma$ Rydberg orbitals for hexatriene. Orbitals a, c, e use basis set A, while orbitals b, d, f use basis set B (table 1). Long dashes indicate zero amplitude, solid lines and short dashes indicate positive and negative amplitudes, with a spacing of 0.005 atomic units between the contours.

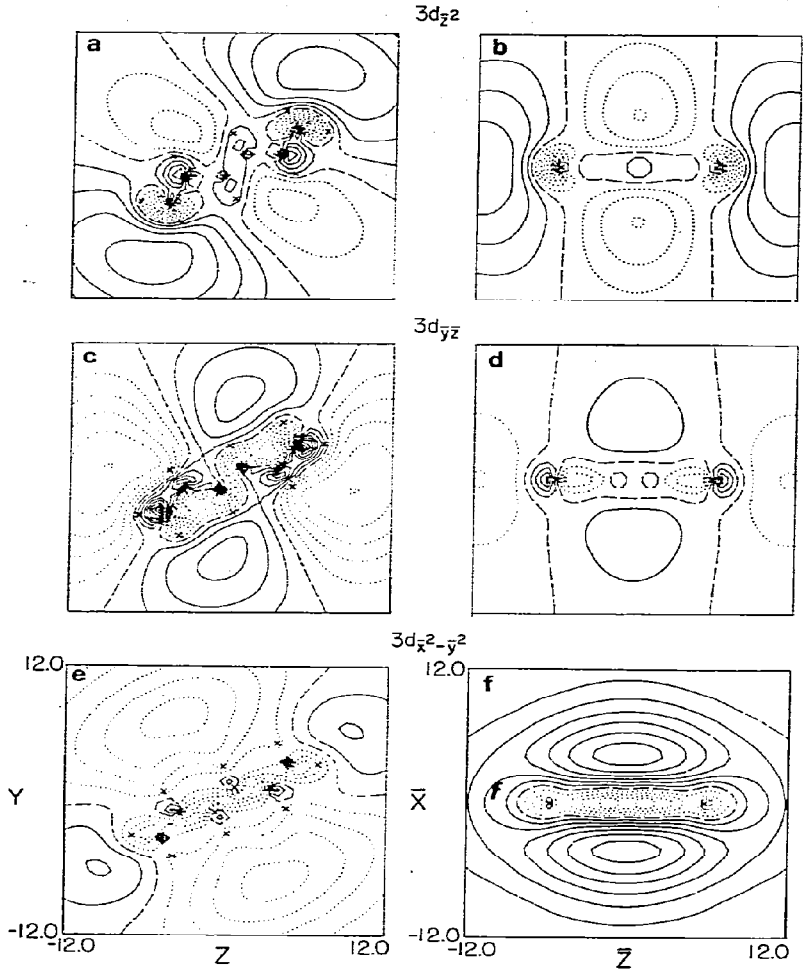

Fig. 2. $3d_\sigma$ Rydberg orbitals for hexatriene. Orbitals a, c, e in the molecular plane. Orbitals b, d, f in the plane perpendicular to the molecule and parallel to the molecular axis ($\bar{z}$). Amplitudes as in fig. 1.

axis of the molecule, but the π Rydberg orbitals seem to be oriented parallel (z axis) and perpendicular (y axis) to the central C_3–C_4 bond.

Figs. 1(a, c, e) shows the first three σ Rydberg orbitals (using basis A) which can be classified relative to the ($\bar{x}$, $\bar{y}$, $\bar{z}$) system (fig. 1) as 3s(a), $3p_{\bar{y}}$(c) and $3p_{\bar{z}}$(e). Similarly, the $3d_\sigma$ orbitals in fig. 2 can be classified as $3d_{\bar{z}^2}$(a, b), $3d_{\bar{y}\bar{z}}$(c, d) and $3d_{\bar{x}^2-\bar{y}^2}$(e, f). This latter orbital shows much more amplitude in the molecular plane than the equivalent one in butadiene.

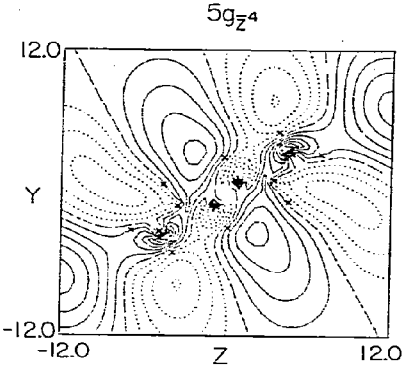

Fig. 3. $5g_{\bar{z}^4}$ Rydberg orbital for hexatriene. Amplitudes as in fig. 1.

Fig. 4 shows the first three π Rydberg orbitals, obtained from basis set C (table 1). Amplitude plots in both xy and $\bar{x}\bar{z}$ planes allow us to classify them as $3d_{xy}$(a, b) and $3d_{\bar{x}\bar{z}}$(c, d). Fig. 5 shows the two 4f orbitals ($4f_{xz^2}$ and $4f_{xy^2}$) in both $\bar{x}\bar{z}$ and xy planes.

Table 2 shows the transition moments and spatial extension (second moments) computed using these Rydberg orbitals.

3.3. Hartree–Fock calculations

For the σ Rydberg states we used the IVO's obtained with basis set B (table 1) as starting guesses for the excited Rydberg orbitals.

Using the first IVO of $a_g(3s)$ symmetry and $b_u(3p_\sigma)$ symmetry we solved self-consistently for the $^1A_u(3s)$ and $^1B_g(3p_\sigma)$ Rydberg states.

For the π Rydberg states we used the IVO's obtained with basis set C (table 1) as starting guesses for the excited Rydberg orbitals.

Similar to the case of butadiene, the Hartree–Fock solution for the $^1A_g(3p_\pi)$ Rydberg state will not correspond to a "pure" state. But because this latter state is very different in character from the valence ^1A_g states it will be easily identified at the CI level, as discussed in the next section.

The ^1B_u states in the case of hexatriene correspond to the nd_π Rydberg states. Using the first IVO of $b_g(3d_\pi)$ symmetry obtained from basis set C (table 2) we solved self-consistently for the $^1B_u(3d_\pi)$ state.

The Hartree–Fock results for the Rydberg states are shown in table 3.

3.4. CI calculations

The set of CI calculations to be described below were performed using the orbitals generated by each one of the SCF calculations respectively, plus some IVO's properly reorthogonalized to the HF occupied orbitals.

For simplicity we limited ourselves to the first two Rydberg states of each symmetry with exception of the ^1A_g states. In that case, the need to project out the ground state and the $2\,^1A_g$ valence state forces us to solve for four roots to obtain the first two ^1A_g Rydberg states.

3.4.1. The ^1A_u states (ns, nd_σ)

The CI calculation for these states was performed in the following way. The π space was formed by the orbitals generated in the SCF calculation. The σ space was formed using the 3s orbital solved self-consistently plus five σ IVO's ($2a_g+3b_u$) obtained from basis set B (table 1), reorthogonalized to the HF σ core. Using these spaces we allowed up to triple excitations among the twelve π MO's while simultaneously allowing the σ electron to readjust among the six σ MO's. The first root of this CI calculation corresponds to the 3s Rydberg state and the second to the $3d_\sigma$ Rydberg state. Both states are optically allowed and should be observed in both UV and electron-impact experiments. The result of this calculation puts the 3s state at 5.97 eV and the first $3d_\sigma$ ($3d_{z^2}$) state at 6.72 eV (table 4).

Although we did solve for the second and third $3d_\sigma$ Rydberg state in the CI calculation one can estimate the location of these states from the IVO calculations corrected by the CI effect observed for the two lower Rydberg states. This puts the second and third $3d_\sigma$ Rydberg state at 6.81 and 7.07 eV.

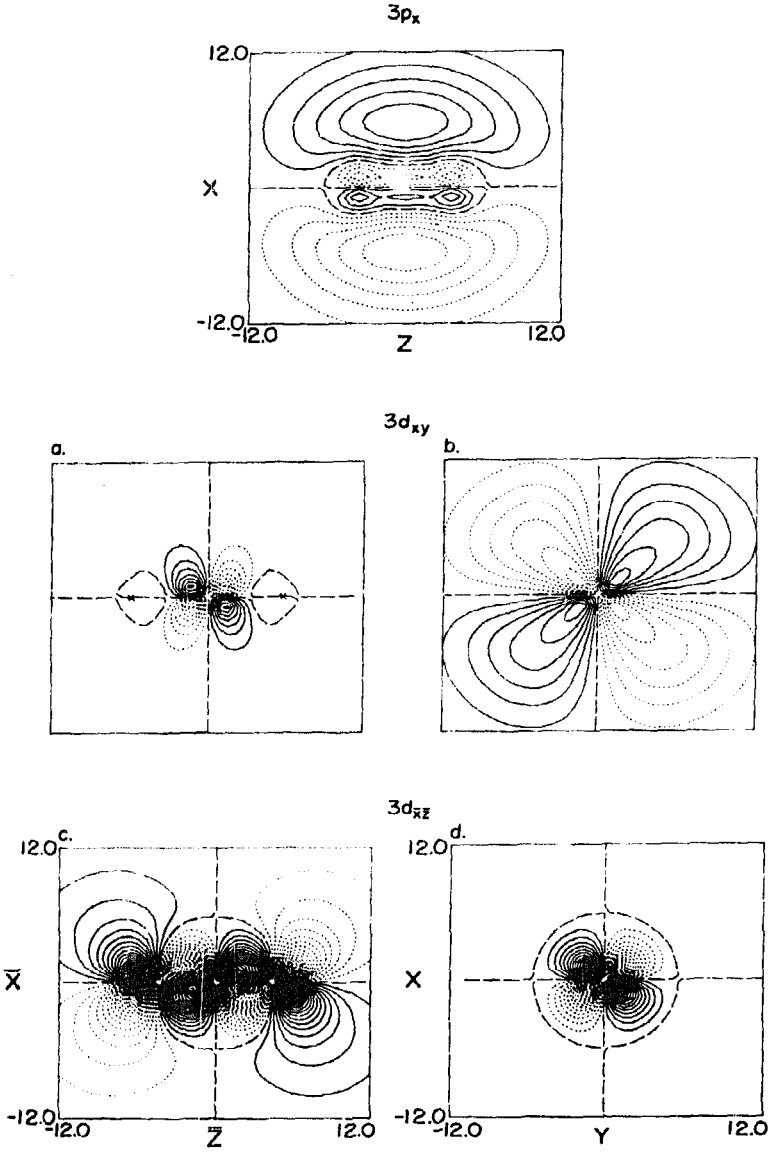

Fig. 4. 3_{p_x} and $3d_{\pi}$ Rydberg orbitals for hexatriene. Orbitals b and d in the xy plane. Orbitals a and c in the $(\bar{x}, \bar{z})$ plane (perpendicular to the molecule). Amplitudes as in fig. 1.

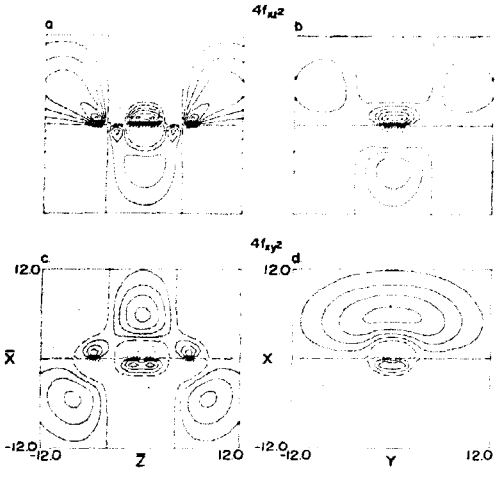

Fig. 5. f_π Rydberg orbitals for hexatriene. Orbitals b and d in the xy plane. Orbitals a and c in the $(\bar{x}, \bar{z})$ plane. Amplitudes as in fig. 1.

3.4.2. The ^1B_g states (np_σ)

The CI calculations for these states were performed analogously to the ^1A_u states.

The π space was formed from the orbitals generated by the SCF calculation. The σ space was formed by the $3p_\sigma$ self-consistently optimized orbital plus five σ IVO's (three a_g + two b_u) properly reorthogonalized to the HF σ orbitals.

Using this space, the CI calculation was performed allowing up to triple excitations among the twelve π MO's and simultaneously allowing the σ electron to readjust among the six σ MO's. The two CI roots obtained correspond to the two $3p_\sigma$ Rydberg states. We found those states at 6.00 eV ($3p_{\bar{y}}$) and 6.20 eV ($3p_{\bar{z}}$).

3.4.3. The ^1A_g states (np_π)

For these states the π space was composed of the HF π orbitals plus six π IVO's (three a_u + three b_g) obtained with basis set C (table 1).

Table 2.
Transition moments and spatial extension of the Rydberg orbitals of hexatriene

Orbital[a]	Transition moments (a_u)		Second moments[c]		
	$\langle\phi_{IVO}\|r^*\|\pi_3(2a_u)\rangle$[b]	component	$\langle x^2\rangle$	$\langle y^2\rangle$	$\langle z^2\rangle$
$\pi_1(1a_u)$			2.525	3.114	8.010
$\pi_2(1b_g)$			2.566	5.799	17.095
$\pi_3(2a_u)$			2.584	5.789	13.523
3s	0.05597	$\langle x\rangle$	15.924	27.918	23.738
$3p_{\bar{y}}$	0.06012	$\langle xy\rangle$	14.053	40.832	22.196
	0.01468	$\langle xz\rangle$			
$3p_{\bar{z}}$	0.70216	$\langle xy\rangle$	22.045	34.738	66.956
	1.40801	$\langle xz\rangle$			
$3p_x$	0.93646	$\langle yz\rangle$	39.436	16.233	17.812
$3d_{z^2}$	0.10274	$\langle x\rangle$	14.998	26.998	82.143
$3d_{\bar{y}z}$	0.15104	$\langle x\rangle$	19.023	68.453	58.839
$3d_{\bar{x}^2-\bar{y}^2}$	0.07412	$\langle x\rangle$	18.707	36.386	28.052
$3d_{\bar{x}\bar{z}}$	1.54968	$\langle y\rangle$	10.866	14.143	24.439
	1.76378	$\langle z\rangle$			
$3d_{xy}$	0.17917	$\langle y\rangle$	30.972	27.246	18.326
	0.22968	$\langle z\rangle$			
$4f_{\bar{x}z^2}$	2.72703	$\langle yz\rangle$	31.744	41.182	41.616
$4d_{\bar{x}\bar{z}}$	0.78711	$\langle y\rangle$	31.764	18.300	39.048
	0.81046	$\langle z\rangle$			
$4f_{x\bar{y}^2}$	0.11374	$\langle yz\rangle$	37.315	13.624	59.284

[a] Orbitals π_1, π_2 and π_3 are from ground state wavefunction. Rydberg orbitals are from IVO calculations.
[b] Transition moments using IVO orbitals. [c] Second moments from IVO orbitals.

Table 3
Hartree–Fock transition energies for the Rydberg states of *trans*-hexatriene

State	Transition energy (eV)
$X\,^1A_g$(−231.72322 hartrees)	
$1\,^1A_u(3s)$	5.38
$1\,^1B_g(3p_y)$	5.29
$^1B_u(3d_{zz})$	5.78

Using this space we performed the CI calculation allowing up to quadruple excitations.

The first root of the CI calculation is a valence closed-shell state corresponding to the $X\,^1A_g$ ground state of the system. The second root is also a valence state and shows the doubly-excited dominant configuration characteristic of the $2\,^1A_g(\pi \rightarrow \pi^*)$ valence state. Finally, the third root corresponds to the diffuse open-shell configuration of the Hartree–Fock calculation and corresponds with the $^1A_g(3p_x)$ Rydberg state. We found this state at 6.26 eV in excellent agreement with the state at 6.23 eV observed in the two-photon absorption experiment [8].

Table 4
CI transition energies for the Rydberg states of *trans*-hexatriene

State	Transition energy (eV)
$3s(1\,^1A_u)$	5.97
$3p_y(1\,^1B_g)$	6.00
$3p_z(2\,^1B_g)$	6.20
$3p_x(3\,^1A_g)$	6.26
$3d_{zz}(^1B_u)$	6.27
$3d_{xy}(^1B_u)$	6.68
$3d_{x^2}(2\,^1A_g)$	6.72
$3d_{yy}(3\,^1A_u)$	6.86[a]
$4f_{xz^2}(4\,^1A_g)$	7.19[a]
$4f_{zy^2}(5\,^1A_g)$	7.81[a]

[a] Estimated by correcting IVO results for CI effects found in lower Rydberg states.

The IVO calculations for the higher ^1A_g Rydberg states were corrected for CI effects found in the $^1A_g(3p_x)$ state (as for the $3d_\sigma$ Rydberg states). The result is the $4f_{xz^2}$ state at 7.19 eV and the $4f_{zy^2}$ state at 7.81 eV.

3.4.4. The ^1B_u states (nd_π)

The CI calculations for these states were carried out in exactly the same way as described for the ^1A_g states. The π space was formed using the HF π orbitals for the ^1B_u state plus six π IVO's (three a_u + three b_g) reorthogonalized to the HF π orbitals. Using this space we solved for two CI roots allowing up to quadruple excitations. These two roots correspond to the two $3d_\pi$ orbitals. We found these states at 6.27 eV and 6.68 eV.

We also estimated the transition energy for the $4d_\pi$ Rydberg state following the same procedure used for the $3d_\sigma(^1A_u)$ states. In this way we obtained a transition energy of 7.41 eV for the $4d_{zz}$ state which correlates well with the transitions observed experimentally at 7.46–7.48 eV [2, 5].

4. Discussion

Unambiguous spectral assignments have been made only for the two lowest triplet states ($1\,^3B_u$ and $1\,^3A_g$), the $1\,^1B_u(\pi \rightarrow \pi^*)$ state and the $^1A_g(\pi_u \rightarrow 3p)$ state. From our calculations we can now provide a quantitative assignment for most of the observed transitions. Table 5 shows the complete results of our calculations and compares them with the available experimental results.

The two lowest observed transitions at ≈2.6 eV and ≈4.2 eV have been assigned to the first two triplet states [5, 14, 25]. Our calculation confirms the assignments. We find the $1\,^3B_u$ state at 2.71 eV and the $1\,^3A_g$ state at 4.35 eV.

The next experimentally observed transition corresponds to the strong dipole-allowed $1\,^1B_u$ state [2b, 5, 14]. Similar to the butadiene case, this is a very broad band covering the range from ≈4.95 eV to ≈5.70 eV.

Table 5.
Excited electronic states of the all-*trans* hexatriene molecule

State[a]	Theoretical results (eV)[b] (present work)	Experimental results (eV)		
		Gabin and Rice[c]	Flicker et al.[d]	others
$1\,^3B_u$	2.71		2.61 (1.9–3.5)	2.58[e]
$1\,^2A_g$	4.32		4.11 (3.6–4.6)	4.2[f]
$1\,^1B_u(\pi\rightarrow\pi^*)$		4.93	4.95, 5.13, 5.5, 5.7	(5.1–5.7)[f]
$2\,^1A_g(\pi\rightarrow\pi^*)$	5.87			
$1\,^1A_u(3s)$	5.97	5.94 ($2\,^1A_g$, $2\,^1B_u$, $3\,^1A_g$)	6.06	
$1\,^1B_g(3p_y)$	6.00[g]			
$2\,^1B_g(3p_z)$	6.20[g]			
$3\,^1A_g(3p_x)$	6.26			6.23[h]
$^1B_u(3d_{zz})$	6.27	6.28 ($2\,^1A_g$, $3\,^1A_g$, $2\,^1B_u$)	6.25	6.2[f]
$^1B_u(\pi\rightarrow\pi^*)$ valence	6.56	6.53 ($2\,^1B_u$)	6.57	
$^1B_u(3d_{xy})$	6.68	6.68		
$2\,^1A_u(3d_{z^2})$	6.72	6.73 ($2\,^1B_u$, ν_2)	6.75	
$3\,^1A_u(3d_{yz})$	6.81[i]	6.90 ($2\,^1B_u$, ν_1)	6.93	6.9[f]
$4\,^1A_u(3d_{x^2-y^2})$	7.07[i]	7.06 ($2\,^1B_u$, $\nu_2+\nu_5$)	7.08	
$^1B_u(4d_{zz})$	7.25	7.26 ($2\,^1B_u$, $\nu_1+\nu_2+\nu_3$)	7.25	
$^1B_u(4d_{xy})$	7.42	7.37		
$^1A_u(4d_{z^2})$	7.44	7.48		
$^1B_u(5d_{zz})$	7.68	7.68		
$^1A_u(5d_{z^2})$	7.75	7.71 ($5p_x$)[j]	7.77	
$^1B_u(5d_{xy})$	7.76			
$^1B_u(6d_{zz})$	7.90	7.88 ($6p_x$)	7.93	
$^1B_u(6d_{xy})$	7.93	7.98 ($7p_x$)		
$^1A_u(6d_{z^2})$	7.94			
$^1B_u(7d_{zz})$	8.01	8.05 ($8p_x$)	8.06	8.0[f]
$^1B_u(7d_{xy})$, $^1A_u(7d_{z^2})$	8.04			
$^1B_u(8d_{zz})$	8.09	8.10 ($9p_x$)		
$^1B_u(8d_{xy})$, $^1A_u(8d_{z^2})$	8.11			
9d	8.18	8.13 ($10p_x$)		
10d	8.21	8.15 ($11p_x$)		
11d	8.23	8.17 ($12p_x$)		
∞d	8.33	8.27 (∞p_x)		
$^1B_g(\sigma\rightarrow\pi^*)$	9.18		9.1	9.2[f]
			9.7	9.6[f]
			10.5	10.7[f]
$^1A_u(\sigma\rightarrow\pi^*)$	11.51			

[a] State assignments based on present calculations, except for the $1\,^1B_u(\pi\rightarrow\pi^*)$ transition.
[b] Valence states are from paper I.
[c] Ref. [2]. Assignments in this column from refs. [2, 26].
[d] Ref. [5]. [e] Ref. [25]. [f] Ref. [14].
[g] These transitions are probably not observed. See text for discussion. [h] Ref. [8].
[i] These are estimated values from IVO calculations plus CI corrections. See text for discussion.
[j] All members of this series computed using Rydberg formula in ref. [2].

The next transition observed in the UV spectrum corresponds to a series of weak bands covering the range from ≈ 5.70 eV to 6.44 eV. These transitions correlate with the bands at 6.06, 6.25 and 6.42 eV observed in the electron-impact experiment [5]. From the analysis of the UV spectrum it was found that only a few of these bands could be fitted in the progressions found for the $X\,^1A_g \rightarrow 1\,^1B_u$ transition, even if rather large anharmonicities are

assumed for the vibrations [2]. From that observation it was concluded that the majority of the observed bands in this region could well be associated with electronic states other than the $1\,^1B_u$ state. These transitions were previously assigned to the parity-forbidden $2\,^1A_g$ and $3\,^1A_g$ states [2] and more recently to an optically allowed $2\,^1B_u$ state [26].

The first state predicted by our calculations to occur in this region is the valence $2\,^1A_g$ state at 5.47 eV*. This $2\,^1A_g$ state could well be associated with the weak bands in the region between 5.70 eV and 5.89 eV of the UV spectrum. The electron-impact spectrum at 70° shows a weak feature at ≈ 5.9 eV which is not present in the spectrum at 0° angle [5]. Since optically forbidden transitions are in general more prominent at larger scattering angles, that feature could be an indication of the ^1A_g parity-forbidden transition. However, this observation is far from being conclusive. Besides the fact that the two spectra have different resolution, several factors could contribute to simulate such a weak feature. A more convenient way of verifying the presence of this state would be by means of a two-photon absorption experiment. To have an idea of how strong this transition would be, we calculated the two-photon transition rate for the $X\,^1A_g \rightarrow 2\,^1A_g$ transition using our best CI description of these states. We found transition rates equal to $3.4\times10^{-50}\ F^2\ s^{-1}$ for the case of linearly polarized light and $4.9\times10^{-50}\ F^2\ s^{-1}$ for the case of circularly polarized light (F is the photon flux in photons/cm^2 s)†. Since fluxes of the order of 10^{25}–10^{26} are currently available (from nitrogen-pumped dye lasers for instance) the transition should be observable.

In the same region (5.70–6.44 eV) our calculations predict two optically allowed Rydberg states and three parity-forbidden Rydberg states. The first transition, at 5.97 eV, corresponds to the $1\,^1A_u$ 3s Rydberg state. This state could well be associated with the bands in the region of 5.94–6.09 eV in the UV [2] spectrum and with the 6.06 eV feature of the electron-impact spectrum [5]. The next three transitions calculated in this region correspond to parity forbidden Rydberg states at 6.00 eV (^1B_g, $3p_y$), at 6.20 eV ($2\,^1B_g$, $3p_z$) and at 6.26 eV ($3\,^1A_g$, $3p_x$).

These Rydberg states occur in the same region as optically allowed transitions and could well be masked by these transitions. Also in the electron-impact spectrum at 0° angle, these transitions should exhibit small cross sections. A recent two-photon absorption experiment indicated the presence of a parity-forbidden state [8], in the region of 6.00 to 6.70 eV. A more recent study of its intensity dependence on the laser beam polarization indicated a state of A_g symmetry [9] at 6.23 eV, in excellent agreement with our calculated $3\,^1A_g(3p_x)$ Rydberg state. But this same experiment [8] does not show the presence of ^1B_g states at 6.00 eV and 6.20 eV. Calculations of the two-photon transition rates for both ^1A_g and ^1B_g Rydberg states (using IVO states to perform the summation over the intermediate states) led us to transition rates for the ^1A_g state relative to the ^1B_g states of ≈ 6 for linearly polarized light and ≈ 10 for circularly polarized light. Similar calculations for butadiene suggest that such IVO calculations may underestimate the ratio of the ^1A_g to ^1B_g by a factor of ≈ 5. Thus the ^1A_g transition might be ≈ 30–50 times more intense than the ^1B_g transitions. In conclusion, the ^1B_g Rydberg states would have been difficult to detect in the two-photon experiment [8], mainly the $^1B_g(3p_z)$ at 6.20 eV, masked by the more intense ^1A_g state at 6.26 eV. It is interesting to notice that those same transitions ($\pi \rightarrow 3p_\sigma$) in butadiene [20] (in which case they are optically allowed) are also weak and one of them is

* Earlier semi-empirical calculations [27] predicted this state to occur below the $1\,^1B_u$ state. This order is an artifact of the semi-empirical method. The analysis of both UV [2] and electron-impact [5] spectra does not show any evidence for such a state below the $1\,^1B_u$ state.

† In paper II these numbers were misprinted ($7.1\times10^{-51}\ F^2\ s^{-1}$ for linearly polarized light and $1.2\times10^{-[illegible]}\ F^2\ s^{-1}$ for circularly polarized light). Also the transition rates for the $X\,^1A_g \rightarrow 3\,^1A_g(3p_x)$ were misprinted. The correct values for the latter transition are: $0.9\times10^{-[illegible]}\ F^2\ s^{-1}$ and $1.9\times10^{-52}\ F^2\ s^{-1}$ for circularly and linearly polarized light, respectively. The ratios for the transitions to the ^1A_g and ^1B_g Rydberg states are correct.

almost certainly not observed. Finally, the last transition in this region predicted by our calculations occurs at 6.27 eV and corresponds to the $^1B_u(3d_{zz})$ Rydberg state. This transition can be correlated with the bands at 6.28 eV in the UV [2] spectrum and at 6.25 eV in the electron-impact spectrum [5]. We found no other transitions at higher energies in this region that could be correlated to the bands observed at 6.38–6.44 eV in the UV [2] spectrum and with the peak at 6.42 eV in the electron-impact spectrum [5].

In one reinterpretation of the UV spectrum this whole system of bands (5.70–6.44 eV) was assigned to a $2\,^1B_u$ state [26]. From our calculations it is clear that more than a single transition is present in this region.

The next band system observed in the UV spectrum corresponds to a series of medium intensity bands covering the range between 6.53 eV and 7.30 eV [2]. This band system was initially assigned to a $2\,^1B_u$ state [2] and more recently to a $\sigma \rightarrow \pi^*\,^1A_u$ state [26]. The corresponding peaks in the electron-impact spectrum are observed at 6.57, 6.75, 6.93, 7.08, and 7.25 eV [5]. In this region (6.53–7.30 eV) we found several transitions which we now will analyze.

The first calculated transition in this region corresponds to a ^1B_u *valence* state at 6.56 eV, close to the observed transition at 6.53 eV. If we assume that the last few bands (at 6.38 eV and 6.44 eV) of the previous region (5.70–6.44 eV) are hot bands $[-2\nu_5, -2(\nu_5-\nu_6)]$ of the observed transition at 6.53 eV (0–0) [2], we could assign the band system (6.42–6.52 eV) to the ^1B_u *valence* state. However, we must be cautious in such an assignment because of uncertainties in the accuracy of our ^1B_u calculation due to mixing of ^1B_u Rydberg and valence states.

The next state predicted to occur in this region corresponds to the $^1B_u(3d_{xy})$ Rydberg state calculated at 6.68 eV. A transition at the same energy observed in the UV spectrum was assigned to a vibronic (ν_3) transition of the 6.53 eV band (0–0) [2]. We found another Rydberg state at 6.72 eV corresponding to the $2\,^1A_u(3d_{\bar{x}^2})$ state. This state can be associated with the transition observed at 6.73 eV in the UV spectrum [2] and with the one at 6.75 eV in the electron-impact spectrum [5]. The next two transitions calculated at $\approx$6.81 eV and $\approx$7.07 eV correspond to the $3\,^1A_u(3d_{\bar{y}\bar{z}})$ and $4\,^1A_u(3d_{\bar{x}^2-\bar{y}^2})$ Rydberg states, respectively. The transition at 6.81 eV can be correlated to the observed transition at 6.90 eV in the UV spectrum [2] and the one at 6.93 eV in the electron-impact spectrum [5]. Similarly the $4\,^1A_u(3d_{\bar{x}^2-\bar{y}^2})$ state can be correlated with the transition at 7.06 eV (UV) [1] and 7.08 eV (EI) [5].

The last state predicted by our calculations to occur in this region corresponds to the $^1B_u(4d_{\bar{x}\bar{z}})$ Rydberg state at 7.25 eV. This state could be associated with the bands observed at 7.15–7.30 eV in the UV spectrum [2] and with the peak at 7.25 eV of the electron-impact spectrum [5]. This transition was experimentally assigned to a vibronic component of the $2\,^1B_u(\pi \rightarrow \pi^*)$ state [2].

A series of medium intensity bands starting from $\approx$7.37 eV to 7.68 eV in the UV spectrum have been tentatively assigned to a $3\,^1B_u$ state [2] or to a $\sigma \rightarrow \pi^*$ state [26]. From paper I [18] we know that this transition does not correspond to a $\sigma \rightarrow \pi^*$ state. Only one transition at 7.48 eV is observed in the electron-impact spectrum [5]. In this region our calculations predict Rydberg states at 7.42 eV$(4d_{xy})$, 7.44 eV$(4d_{\bar{z}^2})$ and 7.68 eV$(5d_{xy})$.

A final series of sharp bands starting at $\approx$7.71 eV and extending up to 8.30 eV is observed in the UV spectrum [2]. The associated transitions in the electron-impact spectrum are found at 7.77, 7.93, and 8.06 eV [5]. The analysis of the UV spectrum revealed that these transitions could be fitted in a p_π-type Rydberg series with the principal quantum number in the range $n = 5, 12$ and quantum defect equal to 0.054 [2].

To understand the nature of these transitions, we examined the various Rydberg series for which our calculations provided the first members. Table 6 shows the results of our studies on four Rydberg series. From table 6 we can see that:

Table 6.
Rydberg series for the hexatriene molecule[a)]

n	$ns(^1A_u)$ $\delta=0.6$	$nd_{z^2}(^1A_u)$ $\delta=0.09$	$nd_{xz}(^1B_u)$ $\delta=0.43$	$nd_{xy}(^1B_u)$ $\delta=0.13$
3	5.97[b)]	6.72[b)]	6.27[b)]	6.68[b)]
4	7.15	7.44	7.26	7.42
5	7.63	7.76	7.68	7.75
6	7.86	7.94	7.90	7.93
7	7.99	8.04	8.01	8.04
8	8.08	8.11	8.09	8.11
9	8.13	8.16	8.14	8.16
10	8.17	8.19	8.18	8.19
11	8.20	8.21	8.21	8.21
12	8.22	8.23	8.23	8.23
∞	8.33	8.33	8.33	8.33

a) All energies in eV.
b) First members of the series are calculated values. Higher members are predicted values based on the quantum defect.

(a) except for d_{z^2} the quantum defects obtained are in the range expected for each type of series [28]*;

(b) for $n \geq 4$, the nd_{z^2} and nd_{xy} series are practically degenerate and for $n \geq 10$ all the nd series are degenerate. Also, for $n \geq 11$ the four series are practically degenerate; and

(c) these four optically allowed series can account for all the transitions observed in this region.

From the results of our analysis we conclude that the series of bands starting at 7.71 eV and converging to the first IP should correspond to three nd Rydberg series. The first member of the nd_{z^2} series is more intense than the first members of the other series. This difference in intensity could imply that for large n all the transitions should correspond to members of this series (nd_{z^2}). Higher members of the ns series are not expected to be observed because the $3s(^1A_u)$ transition is very weak.

Our assignments for this region are shown in table 5. The disagreement between our theoretical transitions and the observed transitions for larger values of n ($n \geq 9$) is certainly due to the fact that the experimental series [2] converges to an IP lower than the one obtained in the photoelectron spectra [29].

Finally, in the electron-impact spectrum [5], transitions corresponding to super-excited states are observed at 9.1 eV, 9.7 eV and 10.5 eV. The transitions can be associated with $\sigma \rightarrow \pi^*$ transitions or with transitions from the inner $\pi(1b_g)$ orbital. The transition at 9.1 eV correlates well with the $^1B_g(\sigma \rightarrow \pi^*)$ state calculated at 9.18 eV. We did not find any transitions that could be correlated with the ones observed at 9.7 eV and 10.5 eV. Those latter states could correspond either to another $^1B_g(\sigma \rightarrow \pi^*)$ state (the 10.5 eV transition most probably) or to transitions from the inner $\pi(1b_g)$ orbital.

Above 11 eV (energy loss) the electron-impact spectra do not show enough resolution to allow for the identification of the $^1A_u(\sigma \rightarrow \pi^*)$ state predicted by our calculation to occur at 11.51 eV.

* The d_{z^2} transition leads to a ^1B_u state that can couple with the $\pi \rightarrow \pi^*$ ^1B_u state (see fig. 4c for a plot of the d_{z^2} orbital). This coupling leads to a higher than usual quantum defect (0.43 rather than 0.1) and may cause the higher levels to be shifted from the values expected from the Rydberg formula.

5. Summary

Most of the results obtained could be predicted from similar calculations performed in the butadiene molecule. As in butadiene [20]:

(a) the spectrum of the hexatriene molecule can be understood in terms of a few valence states plus a series of Rydberg states;

(b) to accurately describe the π-Rydberg states, it is not necessary to include σ correlation;

(c) in the description of the σ Rydberg states the size of the basis set can be considerably reduced without loss of accuracy by using appropriate off-center basis functions.

We believe that some understanding about the nature of the excited states of these molecules has been gained from these calculations. From what was learned, larger systems can be treated, and a pattern of how the structure of the spectrum changes with increasing chain length can be established. Work in this direction is in progress.

Acknowledgement

This work was supported by grants from the National Science Foundation (CHE73-05132) and the NIH (GM-23971) National Institute of General Medical Sciences. Computing assistance was obtained from the Health Sciences Computing Facility of the University of California, Los Angeles, supported by the National Institutes of Health, Research Resources Grant RR-3.

References

[1] B. Hudson and B. Kohler, Ann. Rev. Phys. Chem. 25 (1974) 435, and references therein.
[2] R.M. Gavin Jr. and S.A. Rice, J. Chem. Phys. 60 (1964) 3231;
R.M. Gavin Jr., S. Risemberg and S.A. Rice, J. Chem. Phys. 58 (1973) 3160.
[3] R. McDiarmid, J. Chem. Phys. 64 (1976) 514;
K.K. Innes and R. McDiarmid, J. Chem. Phys. 68 (1978) 2007.
[4] O.A. Mosher, W.M. Flicker and A. Kuppermann, J. Chem. Phys. 59 (1973) 6502;
W.M. Flicker, O.A. Mosher and A. Kuppermann, Chem. Phys. 30 (1978) 307;
A. Kuppermann, W.M. Flicker and O.A. Mosher, Chem. Rev. 79 (1979) 77.
[5] W.M. Flicker, O.A. Mosher and A. Kuppermann, Chem. Phys. Letters 45 (1977) 492.
[6] D.E. Post Jr., W.M. Hetherington III and B. Hudson, Chem. Phys. Letters 35 (1975) 259.
[7] P.J. Johnson, J. Chem. Phys. 64 (1976) 4638.
[8] D.H. Parker, S.J. Sheng and M.A. El-Sayed, J. Chem. Phys. 65 (1976) 5534.
[9] D.H. Parker, J.O. Berg and M.A. El-Sayed, Chem. Phys. Letters, 56 (1978) 197.
[10] D.H. Parker, J.O. Berg and M.A. El-Sayed, in: Advances in laser chemistry, ed. A. Zewail (Springer Series in Chemical Physics, 1978) p. 319.
[11] J.P. Doering, J. Chem. Phys. 70 (1979) 3902.
[12] J.H. Moore Jr., J. Phys. Chem. 76 (1972) 1130.
[13] C. Sandorfy, J. Mol. Struct. 19 (1973) 183.
[14] F.W.E. Knoop and L.J. Oosterhoff, Chem. Phys. Letters 22 (1973) 247.
[15] R.P. Frueholz and A. Kuppermann, J. Chem. Phys. 69 (1978) 3433.
[16] B. Honig and T. Ebrey, Ann Rev. Biophys. Bioeng. 3 (1974) 151;
R.A. Morton and F.A. Pitt, Advan. Enzymol. Related Subj. Biochem. 32 (1969) 97.
[17] D. Oesterhelt, Angew. Chem. Intern. Ed. 15 (1976) 17.
[18] M.A.C. Nascimento and W.A. Goddard III, Chem. Phys. 36 (1979) 147 (paper I).
[19] M.A.C. Nascimento and W.A. Goddard III, Chem. Phys. Letters 60 (1979) 197 (paper II).
[20] M.A.C. Nascimento and W.A. Goddard III, Chem. Phys. 53 (1980) 251 (paper III).
[21] T.H. Dunning Jr. and P.J. Hay, in: Modern theoretical chemistry: Methods of electronic structure theory, Vol. 3, ed. H.F. Schaefer (Plenum Press, New York, 1977) pp. 1–27.
[22] S. Huzinaga, J. Chem. Phys. 42 (1965) 1293.
[23] M. Traetteberg, Acta Chem. Scand. 22 (1968) 628.
[24] W.J. Hunt and W.A. Goddard III, Chem. Phys. Letters 3 (1969) 414.
[25] D.F. Evans, J. Chem. Soc. London (1960) 1735.
[26] M. Karplus, R.M. Gavin Jr. and S.A. Rice, J. Chem. Phys. 63 (1975) 5507.
[27] K. Shulten and M. Karplus, Chem. Phys. Letters 14 (1972) 305.
[28] A.D. Walsh, J. Phys. Radium 15 (1954) 501.
[29] E.E. Astrup, H. Boek, K. Wittel and P. Heimbach, Acta Chem. Scand. A29 (1975) 827.